



MICRO REPORT

Open Access



# Single-molecule imaging of Tau reveals how phosphorylation affects its movement and confinement in living cells

Pranesh Padmanabhan<sup>1\*</sup> , Andrew Kneynsberg<sup>1</sup>, Esteban Cruz<sup>1</sup>, Adam Briner<sup>1</sup> and Jürgen Götz<sup>1\*</sup> 

## Abstract

Tau is a microtubule-associated protein that is regulated by post-translational modifications. The most studied of these modifications is phosphorylation, which affects Tau's aggregation and loss- and gain-of-functions, including the interaction with microtubules, in Alzheimer's disease and primary tauopathies. However, little is known about how Tau's phosphorylation state affects its dynamics and organisation at the single-molecule level. Here, using quantitative single-molecule localisation microscopy, we examined how mimicking or abrogating phosphorylation at 14 disease-associated serine and threonine residues through mutagenesis influences the behaviour of Tau in live Neuro-2a cells. We observed that both pseudohyperphosphorylated Tau (Tau<sup>E14</sup>) and phosphorylation-deficient Tau (Tau<sup>A14</sup>) exhibit a heterogeneous mobility pattern near the plasma membrane. Notably, we found that the mobility of Tau<sup>E14</sup> molecules was higher than wild-type Tau molecules, while Tau<sup>A14</sup> molecules displayed lower mobility. Moreover, Tau<sup>A14</sup> was organised in a filament-like structure resembling cytoskeletal filaments, within which Tau<sup>A14</sup> exhibited spatial and kinetic heterogeneity. Our study provides a direct visualisation of how the phosphorylation state of Tau affects its spatial and temporal organisation, presumably reflecting the phosphorylation-dependent changes in the interactions between Tau and its partners. We suggest that alterations in Tau dynamics resulting from aberrant changes in phosphorylation could be a critical step in its pathological dysregulation.

**Keywords** Tau, Super-resolution microscopy, Phosphorylation, Single-molecule imaging, Microtubules, Tauopathies, Alzheimer's disease

Aberrant changes in the phosphorylation state of the protein Tau characterise a range of neurodegenerative disorders, including Alzheimer's disease and frontotemporal dementia. This hyperphosphorylation is linked to an impairment of neuronal function and eventually, neurodegeneration. Mutagenesis studies have provided valu-

able insights into the effect of Tau phosphorylation on its subcellular localisation, as well as its spreading, release and aggregation in a disease context [1–4]. For instance, pseudohyperphosphorylation of Tau has been shown to decrease the protein's ability to interact with microtubules [2], drive its enrichment in dendritic spines [1, 5], increase its release at the plasma membrane through unconventional secretion pathway [6], and alter the location of the axon initial segment, thereby impairing neuronal excitability [3]. However, how the phosphorylation of Tau affects its behaviour at the single-molecule level is only poorly understood.

\*Correspondence:

Pranesh Padmanabhan  
p.padmanabhan@uq.edu.au  
Jürgen Götz  
j.goetz@uq.edu.au

<sup>1</sup>Clem Jones Centre for Ageing Dementia Research, Queensland Brain Institute, The University of Queensland, 4072 Brisbane, Australia



© The Author(s) 2024. **Open Access** This article is licensed under a Creative Commons Attribution 4.0 International License, which permits use, sharing, adaptation, distribution and reproduction in any medium or format, as long as you give appropriate credit to the original author(s) and the source, provide a link to the Creative Commons licence, and indicate if changes were made. The images or other third party material in this article are included in the article's Creative Commons licence, unless indicated otherwise in a credit line to the material. If material is not included in the article's Creative Commons licence and your intended use is not permitted by statutory regulation or exceeds the permitted use, you will need to obtain permission directly from the copyright holder. To view a copy of this licence, visit <http://creativecommons.org/licenses/by/4.0/>. The Creative Commons Public Domain Dedication waiver (<http://creativecommons.org/publicdomain/zero/1.0/>) applies to the data made available in this article, unless otherwise stated in a credit line to the data.

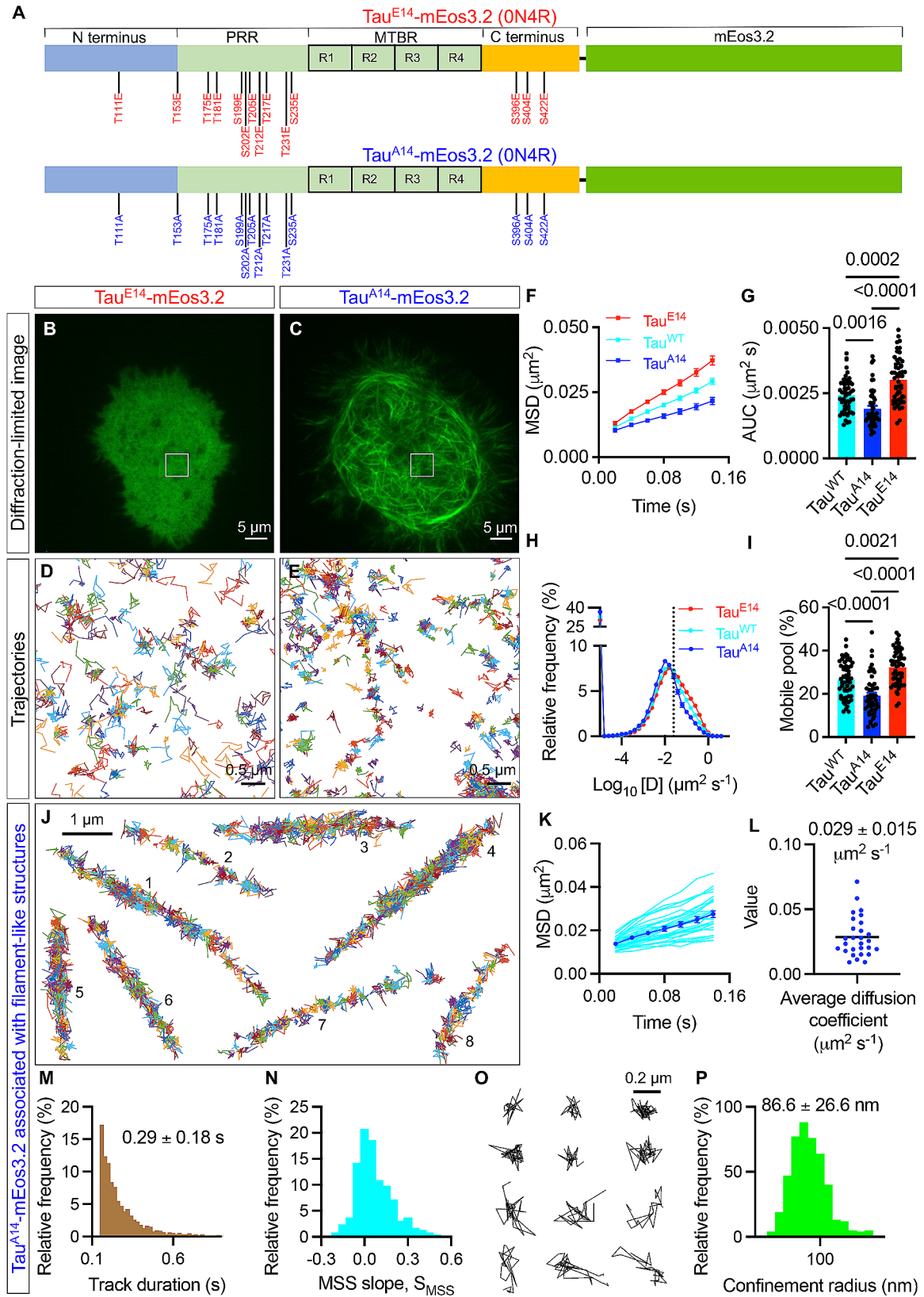


**Fig. 1** (See legend on next page.)

(See figure on previous page.)

**Fig. 1** Tau phosphorylation at 14 residues increases the mobility of Tau near the plasma membrane. A, Schematic of 0N4R Tau tagged with mEos3.2 at the C-terminus with 14 critical Ser/Thr residues replaced by glutamic acid (Tau<sup>E14</sup>-mEos3.2) or alanine (Tau<sup>A14</sup>-mEos3.2). B, C, Representative diffraction-limited TIRF image of N2a cells expressing Tau<sup>E14</sup>-mEos3.2 (B) or Tau<sup>A14</sup>-mEos3.2 (C) acquired in the green channel before sptPALM imaging. D, E, Maps of trajectories of Tau<sup>E14</sup>-mEos3.2 and Tau<sup>A14</sup>-mEos3.2 molecules corresponding to the boxed region shown in panels B and C, respectively. F–I, Comparison of Tau<sup>WT</sup>-mEos3.2, Tau<sup>E14</sup>-mEos3.2 and Tau<sup>A14</sup>-mEos3.2 mobility parameters in live N2a cells. F, G, Average MSD as a function of time (F) and the corresponding area under the curve (AUC) (G). H, J, Distribution of the diffusion coefficients and the corresponding fraction of mobile pool (I). The dashed line indicates the threshold ( $\log_{10}[D] \leq -1.6$ ) demarcating the immobile and the mobile pools of Tau molecules. Error bars, s.e.m. J, Examples of trajectories of Tau<sup>A14</sup>-mEos3.2 molecules associated with filament-like structures. K, L, Average MSD of Tau<sup>A14</sup>-mEos3.2 trajectories associated with filament-like structures (K) and the corresponding average diffusion coefficient (L). M, Distribution of duration of Tau<sup>A14</sup>-mEos3.2 tracks associated with filament-like structures. N, Distribution of the MSS slope,  $S_{MSS}$ , of individual Tau<sup>A14</sup>-mEos3.2 tracks associated with filament-like structures. O, Examples of Tau<sup>A14</sup>-mEos3.2 trajectories associated with filament-like structures classified as immobile or confined pools by MSS analysis. P, Distribution of the confinement radius of immobile and confined pools of Tau<sup>A14</sup>-mEos3.2 molecules from filament-like structures. N=56 cells expressing Tau<sup>WT</sup>-mEos3.2, 49 cells expressing Tau<sup>A14</sup>-mEos3.2, and 55 cells expressing Tau<sup>E14</sup>-mEos3.2 from 5 independent experiments each. In G and I, statistical analysis was performed using one-way ANOVA with the Tukey's multiple comparison correction

To investigate this, we transiently expressed wild-type, phosphomimetic and phosphodeficient forms of the prominent 0N4R isoform of human Tau in murine neuroblastoma Neuro-2a (N2a) cells. Single-molecule imaging was performed using the photoactivatable fluorescent protein mEos3.2, which was fused to the carboxy terminus of Tau. Specifically, we replaced 14 disease-relevant serine and threonine residues with glutamic acid (Tau<sup>E14</sup>-mEos3.2) to mimic hyperphosphorylation, or alanine (Tau<sup>A14</sup>-mEos3.2) to abrogate phosphorylation [1, 3, 5] (Fig. 1A). We then used single-particle tracking photoactivated localisation microscopy (sptPALM) [7] and total internal reflection fluorescence (TIRF) illumination (Fig. S1A) [8] to localise and track individual wild-type (Tau<sup>WT</sup>-mEos3.2) and mutated Tau molecules near the cytosolic leaflet of the plasma membrane with ~100 nm axial resolution (Fig. S1B and S1C). (For more details, see Materials and Methods in Additional File 1.) In this region, Tau assumes its various functions by interacting with its multiple partners: lipids in the plasma membrane, membrane-associated proteins, including the kinase Fyn and the calcium-regulated membrane-binding protein annexin A2, cytoskeletal elements, including the kinase actin filaments and microtubules, and motor proteins, such as dynactin, a co-factor for the cytoplasmic microtubule motor protein dynein-1 [9]. The diffraction-limited TIRF images captured before single-molecule imaging revealed more prominent microtubule filament-like structures in Tau<sup>A14</sup>-mEos3.2-expressing cells compared to those expressing Tau<sup>E14</sup>-mEos3.2 (Fig. 1B, C and Fig. S2). This observation possibly reflects biochemical findings showing a reduction in the association of Tau with microtubules as a result of phosphorylation at these 14 sites [2].

Next, we recorded a time series of detections of either Tau<sup>WT</sup>-mEos3.2, Tau<sup>E14</sup>-mEos3.2 or Tau<sup>A14</sup>-mEos3.2 in the red emission channel (561 nm excitation) at 50 Hz for a duration of 160 s. This allowed us to readily construct thousands of Tau<sup>WT</sup>-mEos3.2, Tau<sup>E14</sup>-mEos3.2 and Tau<sup>A14</sup>-mEos3.2 trajectories per cell (Fig. 1D, E). We first performed a moment scaling spectrum (MSS) analysis

[10] to characterise the mobility pattern of the mutated Tau molecules. As recently observed for Tau<sup>WT</sup>-mEos3.2 [8], both Tau<sup>E14</sup>-mEos3.2 and Tau<sup>A14</sup>-mEos3.2 molecules exhibited a heterogeneous mobility pattern, existing in immobile, confined, and freely diffusive states near the plasma membrane (Fig. S3). We then calculated the average mean square displacement (MSD) and the frequency distribution of the instantaneous diffusion coefficient of all trajectories from each cell (Fig. 1F–I and Fig. S4). The slope of the average MSD curve (Fig. S4) and the area under the average MSD curve (AUC) (Fig. 1F, G) were larger for Tau<sup>E14</sup>-mEos3.2 molecules and smaller for Tau<sup>A14</sup>-mEos3.2 molecules compared to Tau<sup>WT</sup>-mEos3.2 molecules. Moreover, the diffusion coefficient distribution of Tau<sup>E14</sup>-mEos3.2 molecules shifted towards higher values, and the mobile fraction of Tau<sup>E14</sup>-mEos3.2 molecules was significantly higher than that of Tau<sup>WT</sup>-mEos3.2 and Tau<sup>A14</sup>-mEos3.2 molecules (Fig. 1H, I). These observations indicate that Tau<sup>E14</sup>-mEos3.2 molecules are more mobile and Tau<sup>A14</sup>-mEos3.2 molecules are less mobile than wild-type Tau near the plasma membrane in live cells. Notably, we previously found that phosphomimetic mutations at positions 262 and 356 (12E8 epitope) in the microtubule-binding domain, distinct from the 14 mutations that are outside of the microtubule-binding domain and were examined in this study, also increased Tau mobility in N2a cells [8].

In the high-resolution intensity maps of Tau<sup>A14</sup>-mEos3.2 (Fig. S5), we observed signatures of filament-like structures that were also visible in the diffraction-limited TIRF images (Fig. S2) and resembled the well-studied microtubule architecture. We extracted Tau<sup>A14</sup>-mEos3.2 trajectories associated with each of these structures (Fig. 1J and S6) and computed the average MSD curve (Fig. 1K) and the average diffusion coefficient,  $D_{avg}$  (Fig. 1L). We found that the  $D_{avg}$  values varied substantially across the filament-like structures (Fig. 1L) and that the duration of these Tau<sup>A14</sup>-mEos3.2 trajectories was  $0.29 \pm 0.18$  s (mean  $\pm$  s.d.) (Fig. 1M). Moreover, the MSS analysis (Fig. 1N, O) identified individual Tau<sup>A14</sup>-mEos3.2 trajectories associated with

these structures that were immobile and confined, and the confinement radius of the immobile and confined Tau<sup>A14</sup>-mEos3.2 trajectories was  $86.6 \pm 26.6$  nm (mean  $\pm$  s.d.) (Fig. 1P).

In conclusion, our sptPALM approach demonstrated that both Tau<sup>E14</sup> and Tau<sup>A14</sup> molecules are detectable and exhibit heterogeneous mobility patterns close to the cytosolic leaflet of the plasma membrane of N2a cells. Given that the likelihood of tracking free cytosolic Tau molecules under TIRF illumination is low due to their high diffusion coefficient values [11], the observed Tau<sup>E14</sup> and Tau<sup>A14</sup> trajectories are likely to represent molecules that are interacting with the components of the plasma membrane and its associated cytoskeleton. Our results reveal that the mobility of Tau<sup>E14</sup> molecules is significantly higher than that of Tau<sup>A14</sup> molecules. This is probably due to a combination of two factors: the release of Tau<sup>E14</sup> molecules from the microtubules and an increased binding and trapping of Tau<sup>A14</sup> molecules on the microtubules. Recent studies have shown that Tau undergoes unconventional secretion through the plasma membrane in neuroblastoma cells and neurons, and that the Tau<sup>E14</sup> mutant is released to a larger degree than the Tau<sup>A14</sup> mutant in SH-SY5Y neuroblastoma cells [2, 6]. Whether the increased mobility of Tau<sup>E14</sup> molecules observed in our study is causally linked to increased Tau<sup>E14</sup> secretion remains to be tested. The filament-like structures observed in cells expressing Tau<sup>A14</sup>-mEos3.2 presumably represent Tau<sup>A14</sup> molecules associated with microtubules. The duration ( $\sim 0.29$  s) of the Tau<sup>A14</sup>-mEos3.2 trajectories associated with the filament-like structures observed in our study is much longer than the reported dwell time (40 ms) of wild-type 2N4R Tau on microtubules in live PC12 cells [12]. It is plausible that the higher affinity of Tau<sup>A14</sup> towards microtubules could lead to repeated binding and release of Tau<sup>A14</sup> on microtubules, resulting in a longer track duration. Overall, our super-resolution-based approach combined with those of others [2, 12–15] offers a powerful framework to examine the impact of physiological and pathological modifications to Tau on its organisation, behaviour and function in different cellular compartments.

#### Abbreviations

sptPALM	Single-particle tracking photoactivated localisation microscopy
TIRF	Total internal reflection fluorescence
MSS	Moment scaling spectrum
MSD	Mean square displacement
AUC	Area under the curve
D <sub>avg</sub>	Average diffusion coefficient

#### Supplementary Information

The online version contains supplementary material available at <https://doi.org/10.1186/s13041-024-01078-6>.

Supplementary Material 1

#### Acknowledgements

We thank Rowan Tweedale for critical reading of the manuscript. We acknowledge Jean-Baptiste Sibarita, Corey Butler and Adel Kechkar for their contributions in the development of PALM-Tracer.

#### Author contributions

PP, AK and JG designed experiments. PP performed single-molecule imaging and analysis and contributed analytical tools. AK, EC and AB performed cell culture work. PP and JG wrote the manuscript with feedback from AK, EC and AB. All authors discussed the results and approved the final version.

#### Funding

The imaging was performed at the Queensland Brain Institute Advanced Microscopy Facility, supported by the Australian Government through an Australian Research Council LIEF grant (LE130100078). We acknowledge support by the Estate of Dr. Clem Jones, the State Government of Queensland (DSIT), Department of Science, Information Technology and Innovation), and the National Health and Medical Research Council of Australia (GNT1176326 and GA39196) to J.G.

#### Data availability

All data associated with this study are available within the manuscript and its Additional Files.

#### Declarations

##### Ethics approval and consent to participate

Not applicable.

##### Consent for publication

Not applicable.

##### Competing interests

The authors declare that they have no competing interests.

Received: 21 May 2023 / Accepted: 22 January 2024

Published online: 12 February 2024

#### References

1. Hoover BR, Reed MN, Su J, Penrod RD, Kotilinek LA, Grant MK, Pitstick R, Carlson GA, Lanier LM, Yuan LL, et al. Tau mislocalization to dendritic spines mediates synaptic dysfunction independently of neurodegeneration. *Neuron*. 2010;68(6):1067–81.
2. Katsinelos T, Zeitler M, Dimou E, Karakatsani A, Muller HM, Nachman E, Steringer JP, Ruiz de Almodovar C, Nickel W, Jahn TR. Unconventional secretion mediates the trans-cellular spreading of tau. *Cell Rep*. 2018;23(7):2039–55.
3. Hatch RJ, Wei Y, Xia D, Götz J. Hyperphosphorylated Tau causes reduced hippocampal CA1 excitability by relocating the axon initial segment. *Acta Neuropathol*. 2017;133(5):717–30.
4. Hallinan GI, Vargas-Caballero M, West J, Deinhardt K. Tau misfolding efficiently propagates between individual intact hippocampal neurons. *J Neurosci*. 2019;39(48):9623–32.
5. Xia D, Li C, Götz J. Pseudophosphorylation of Tau at distinct epitopes or the presence of the P301L mutation targets the microtubule-associated protein tau to dendritic spines. *Biochim Biophys Acta*. 2015;1852(5):913–24.
6. Merezhko M, Brunello CA, Yan X, Vihinen H, Jokitalo E, Uronen RL, Huttunen HJ. Secretion of Tau via an unconventional non-vesicular mechanism. *Cell Rep*. 2018, 25(8):2027–2035 e2024.
7. Padmanabhan P, Martinez-Marmol R, Xia D, Götz J, Meunier FA. Frontotemporal dementia mutant tau promotes aberrant Fyn nanoclustering in hippocampal dendritic spines. *eLife*. 2019;8:e45040.
8. Padmanabhan P, Kneynsberg A, Cruz E, Amor R, Sibarita JB, Götz J. Single-molecule imaging reveals tau trapping at nanometer-sized dynamic hot spots near the plasma membrane that persists after microtubule perturbation and cholesterol depletion. *EMBO J*. 2022;41(19):e111265.
9. Brandt R, Trushina NI, Bakota L. Much more than a cytoskeletal protein: physiological and pathological functions of the non-microtubule binding region of tau. *Front Neurol*. 2020;11:590059.

10. Jaqaman K, Kuwata H, Touret N, Collins R, Trimble WS, Danuser G, Grinstein S. Cytoskeletal control of CD36 diffusion promotes its receptor and signaling function. *Cell*. 2011;146(4):593–606.
11. Rossier O, Oceau V, Sibarita JB, Leduc C, Tessier B, Nair D, Gatterdam V, Destaing O, Albigès-Rizo C, Tampé R, et al. Integrins  $\beta 1$  and  $\beta 3$  exhibit distinct dynamic nanoscale organizations inside focal adhesions. *Nat Cell Biol*. 2012;14(10):1057–67.
12. Janning D, Igaev M, Sundermann F, Bruhmann J, Beutel O, Heinisch JJ, Bakota L, Piehler J, Junge W, Brandt R. Single-molecule tracking of Tau reveals fast kiss-and-hop interaction with microtubules in living neurons. *Mol Biol Cell*. 2014;25(22):3541–51.
13. Padmanabhan P, Kneynsberg A, Götz J. Super-resolution microscopy: a closer look at synaptic dysfunction in Alzheimer disease. *Nat Rev Neurosci*. 2021;22(12):723–40.
14. Gyparaki MT, Arab A, Sorokina EM, Santiago-Ruiz AN, Bohrer CH, Xiao J, Lakadamyali M. Tau forms oligomeric complexes on microtubules that are distinct from tau aggregates. *Proc Natl Acad Sci U S A* 2021, 118(19).
15. Colom-Cadena M, Davies C, Sirisi S, Kee JE, Simzer EM, Tzioras M, Querol-Vilaseca M, Saánchez-Aced E, Chang YY, Holt K, et al. Synaptic oligomeric tau in Alzheimer's disease — a potential culprit in the spread of tau pathology through the brain. *Neuron*. 2023;111:1–14.

### Publisher's Note

Springer Nature remains neutral with regard to jurisdictional claims in published maps and institutional affiliations.